Journal of Applied Research and Technology

www.jart.icat.unam.mx

ICAT Instituto de Ciencias Aplicadas y Tecnología

Journal of Applied Research and Technology 24 (2026) 354-367

Original

Controlling Some Specifications of Nanofibers Produced by Electrospinning Through the Rotation Speed and Shape of the Collector

Shadi Hossen[1]* • Ghazal Tuhmaz[1] • Kinan Alshaar[2]

[1]Nanofiber Laboratory, Department of Textile Engineering, Faculty of Petroleum and Chemical Engineering, AL Baath University, Homs City, Syria.
[2]Department of Petroleum Engineering, Faculty of Petroleum and Chemical Engineering, AL Baath University, Homs City, Syria

Received: 25 12 2024; Accepted: 30 06 2025
Available: 30 06 2026

Abstract: Nanofibers possess properties that make them suitable for use in a variety of applications, including high specific surface area and biomimetic potential. This has led to numerous potential applications for electrospinning fibers. Precise control and prediction of nanofiber alignment and diameter are critical for these applications. Several variables affect fiber properties, including the collector's speed and shape.

In this research, the conventional collector used in electrospinning technology was modified by using a polyamide collector in the form of a cone-shaped trunk, and the effect of changing the surface inclination angle on the properties of the resulting fibers was studied. The effect of the conical collector's rotational speed on fiber morphology, in terms of diameter alignment and density, was also studied. 5 different rotational speeds were applied within the range of (0-6000) rpm, and three inclination angles of 10, 15, and 30 degrees were tested, with the remaining process parameters held constant.

The results showed that increasing the inclination angle of the surface of the cone increases the diameter of the produced fibers and reduces their density. Regarding the orientation of the fibers, the study showed that high rotational speeds (4500 rpm and above) produced clear parallelism and alignment between the resulting nanofibers and those taken from the base side of the conical collector, with 82% alignment relative to the diameters of the formed fibers. On the

*Corresponding author.
E-mail address: enshadimhosssen@gmail.com (S. Hossen).
Peer Review under the responsibility of Universidad Nacional Autónoma de México.

collector, the results showed that a rotational speed of 3000 rpm gave the smallest fiber diameter, reaching 50.07 nm. Also, samples taken from the base side showed identical results, and the smallest diameter measured was 40.1 nm. By comparing the fiber diameters taken from the two bases of the cone, the results showed the presence of a gradient in the alignment, diameters, and density, allowing the formation of a three-dimensional structure for the resulting fiber network. This study demonstrates the importance of calibrating the rotational speed of the collector and its inclination angle in determining the optimum values to obtain three-dimensional fibers at the nanoscale, which can be used in many potential applications.

Keywords: **conical collector, speed, alignment, fiber diameter, nanofiber, nonwoven, 3d.**

1. Introduction

The first patent for an electrospinning device was granted to Formahls in 1934.

In a typical electrospinning process, a droplet of polymer solution settles on the tip of the needle due to the surface tension of the solution (Reneker et al., 2000; Druesedow, 2008). To initiate electrospinning (Figure 1), a high voltage must be applied to the polymer solution, causing the solution surface to become highly charged. The suspended droplet then elongates and assumes a conical shape known as a Taylor cone, due to the competition between surface tension and the mutual electrostatic repulsion of the surface charges, which counteracts the surface tension (Li & Wang, 2013). When the electric field strength exceeds a threshold, the electrostatic forces overcome surface tension (Rafiei et al., 2013), and a jet forms from the tip of the Taylor cone (Li & Xia, 2004). Disturbances in the jet occur as a result of electrostatic repulsion and interaction with the external electric field, which causes the unstable spiral coiling of the current to begin, which in turn leads to a decrease in the final diameter of the assembled fibers (Reneker et al., 2000; Subbiah et al., 2005).

The variables affecting the electrospinning process, the shape of the final fiber, its diameter, and the presence or absence of knots and defects in the fiber were studied. It was found that the critical element in the electrospinning process is the application of a high voltage to the polymer solution. In general, a high voltage greater than 6 kV can cause the solution to be drawn from the needle tip (Subbiah et al., 2005; Baede, 2009). It was also shown that increasing the solution flow rate increases the fiber diameter when spinning fibers from polystyrene solutions (Haghi, 2009; Haghi, 2010). As the distance between the collector and the needle tip increases, the resulting diameter decreases (Wang et al., 2006).

The rotation speed is an important factor, as it affects the percentage of fibers collected and the diameter of these fibers due to variations in the tension to which they may be exposed (Czaplewski et al., 2004; Kumar, 2012). The collector's rotation speed must be calibrated to match the fiber flow rate. In other words, the rotation speed of the collector determines the degree of fiber regularity and thus affects the fiber diameter (Bosworth & Downes, 2011; Ramakrishna et al., 2005). Precise control and prediction of nanofiber diameter are also crucial for various applications, as polymer concentration, applied voltage, feed rate, collector speed and shape significantly affect nanofiber diameter (Sukpancharoen et al., 2024). Recently, neural inference models have emerged as a means of predicting process variables (Çetinkaya et al., 2024). The most important applications of nanofibers are tissue engineering, flexible electronics and filtration (Zuniga-Navarrete et al., 2024).

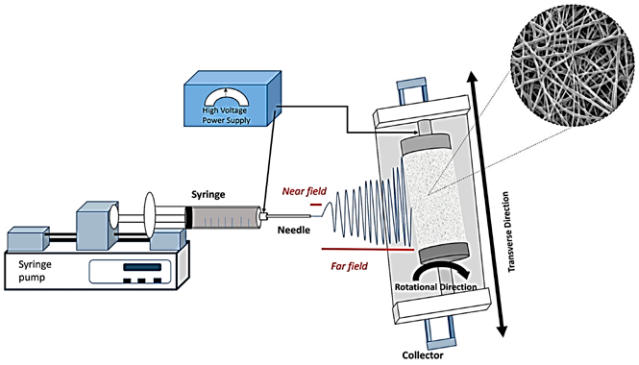

Figure 1. The principle of the electrospinning process (Ahmadi Bonakdar & Rodrigue, 2024).

Controlling fiber orientation is an important step toward many potential uses, but controlling the orientation of electrospinning fibers is not an easy task (Chuangchote & Supaphol, 2006). Several methods have been applied to control fiber orientation, including the use of a high-speed rotating disc (Brown & Stevens, 2007) and gap ring alignment (Rebicek et al., 2011). Oriented networks have been successfully applied to human stem cell culture using electrospinning oriented polycaprolactone (PCL) nanofiber cell carriers, and better cytoskeletal reorganization of stem cells was observed compared to unoriented networks (Lawrencetine & Cato, 2014). "CAMILA. F" also used parallel collagen nanofibers to fabricate artificial knee cartilage. The researcher demonstrated that increasing the parallelism of the fibers and decreasing their diameter can yield artificial cartilage that is functionally similar to natural cartilage (Camilla & Juan, 2016). The ability to control the alignment of silver nanowires could lead to the development of nanoelectronic and nanophotonic structures (Cao et al., 2006).

The shape of the collector also has an important effect on the specifications of the produced fibers. The conical shape of the collector will cause variation in the electrical charge strength, according to Needle (Haider, 2016) (see Figure 2), and the conductive collector reduces charges on the deposited fibers (Ahmadi Bonakdar & Rodrigue, 2024). The cone stem causes a variation in the distance between the extrusion point and the collection points, as well as in the linear velocity of the collector due to the diameter gradient along the forming distance (Bhardwaj & Kundu, 2010) (see Figure 3). In this case, it becomes important to combine the effect of the rotational velocity and the effect of the diameter change of the cone under the term linear velocity and its role in creating a gradient in the structure of the fibers formed on the collector. This gradient will lead to the formation of a three-dimensional fiber network.

Fibers can be described as three-dimensional at the nanoscale in two states: either as nanoparticles or by increasing the surface area-to-volume ratio, which increases the effective surface sites on the fiber network. Creating a gradient in the microstructure of nanofiber networks will increase the number of effective sites. Such networks can be used to improve the growth sites of living cells in tissue engineering (Zhou & Tan, 2017; Cui et al., 2010).

Given the importance of the influence of collector speed on the specifications, homogeneity, alignment, and density of the resulting fibers, the effect of varying the rotational speed of the cone stem on the fiber specifications at different forming points along the collector was studied to achieve optimal values for producing homogeneous fibers with small diameters on the nanometer scale. In a separate step, three types of conical collectors with different inclination angles (10, 15, and 30 degrees) were used, and the effect of the cone inclination angle on the diameter and density of the electrospinning fibers was studied, with the aim of achieving optimal operating conditions for obtaining a three-dimensional Nano network structure.

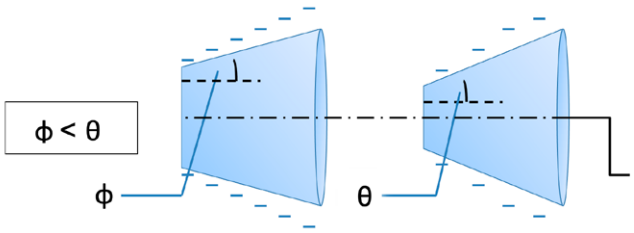

Figure 2. Difference in charge distribution according to the angle of the cone trunk.

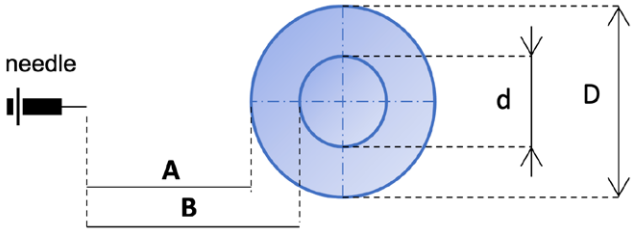

Figure 3. A side view of the conical manifold in a horizontal position, in front of the extrusion needle, shows the difference in diameter and the distance along the complex's length.

2. Materials and Methods

2.1. Materials

During the blow spinning experiments, a solution of poly lactic acid polymer (PLA) was utilized at a concentration of 7% by weight. The solid material of the polymer was obtained from the exhaust of the three-dimensional printing. A mixture of 40% dimethylformamide (DMF) and 60% acetone was used.

2.2. Equipment:

An electrospinning device with an interchangeable collector was used, designed to produce nanofiber webs with multiple specifications (Figure 4). The device was manufactured locally in accordance with the technical specifications shown in Table 1.

Table 1. Technical specifications of the electrospinning device.

Collector rotational speed range	0 – 6000 rpm
Collector reciprocating speed range	12.6 – 25.2 m/min
Polymer pump	ALARIS IVAC P3000
Voltage booster	19-28 Kv, 100 w, 220 v

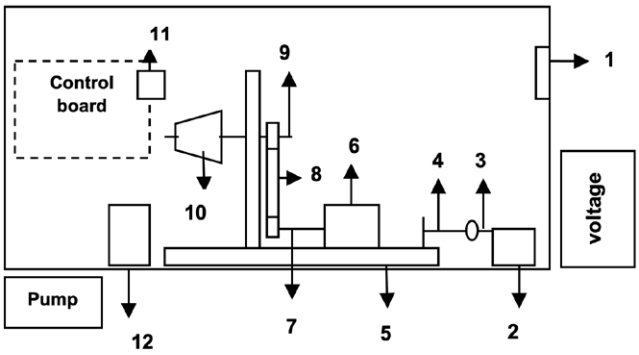

Figure 4. Schematic diagram of the conical electrospinning device.

Figure 4 shows the parts of the device used, where:

1. Cooling fan
2. Reciprocating motor
3. Attached
4. Arm
5. Linear motion track of the complex group
6. Rotary motion engine
7. Motor axis
8. Garlic (peeled)
9. The axis of the collector
10. Conical collector (see Figure 5).
11. Humidity and temperature sensor
12. Humidifier

Table 2. Dimensions of conical collectors.

	θ°	A mm	B mm	C mm	L mm
The first model	10	70	20	8	140
The second model	15	95	20	8	140
The third model	30	182	20	8	140

In Figure 6, the gradient of a cone is defined as the amount of decrease in its diameter after every 1 cm (Equation 1):

$$G = -20.\, L.\, tan\theta \text{ mm} \quad (1)$$

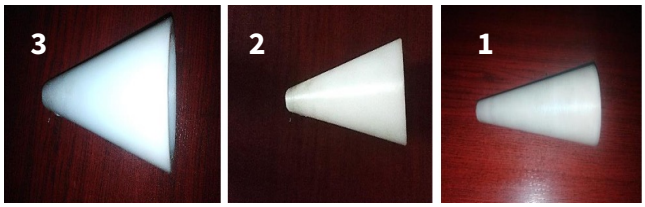

Figure 5. Polyamide conical collectors, 1: 10 degrees, 2: 15 degrees,3: 30-degree inclination.

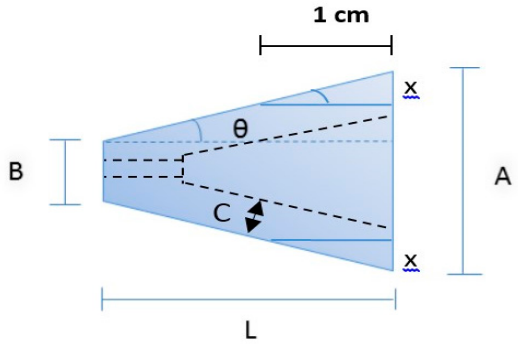

Figure 6. Dimensions of the cone trunk: L: Height of the cone trunk; A: Diameter of the larger base; B: Diameter of the smaller base; C: Thickness of the cone trunk; θ°: Angle of inclination of the cone›s surface from the axis.

The device's operating parameters were adjusted according to previous studies and laboratory experiments. The chamber was conditioned for 30 minutes before starting the electrospinning process to meet the required conditions.

In the first study, the conical collector surface was modified (Table 2), and the effect of collector surface inclination on fiber properties was investigated. Different collector surface inclination angles result in different distributions of electrical charge on the surface and different distances between the needle head and the collector base. In the second study, five rotational speed values were selected, and their effect on properties was studied, while the remaining process parameters were fixed according to Table 3.

The resulting fiber networks were examined using a scanning electron microscope (SEM) model VEGA II XMU. Two samples were taken from different areas of each network: the first sample was collected from the side of the base of the small conical complex, while the second sample was taken from the side of the larger base, at a distance of 1 cm from the edges of the sample, as illustrated in Figure 7.

Table 3. Experimental operating conditions.

PLA solution concentration, %wt	7
Electrical voltage, kv	25
Distance between needle and manifold, cm	18
Solution flow, ml/h	0.1
Operating time, min	60
Humidity, %	60
Temperature, C°	25
The slope angle of the collector surface, degrees	10
	15
	30
Rotational speed of the collector, rpm	0
	1500
	3000
	4500
	6000

Figure 7. Method of selecting samples for microscopic examination.

Microscopic images were analyzed by measuring their diameters, deviations, and densities using reference methods in the ImageJ program (Lawrencetine & Cato, 2014; Zhou & Tan, 2017)

3. Results:

3.1. Effect of Cone Inclination Angle On Fiber Diameter and Density:

In this study, spinning experiments were conducted at a rotational speed of 1500 rpm. Figure 8 shows SEM images of the samples from the great base direction (GBD) and the small base direction (SBD) for each slope angle. Table 4 shows the results of diameter calculations using ImageJ.

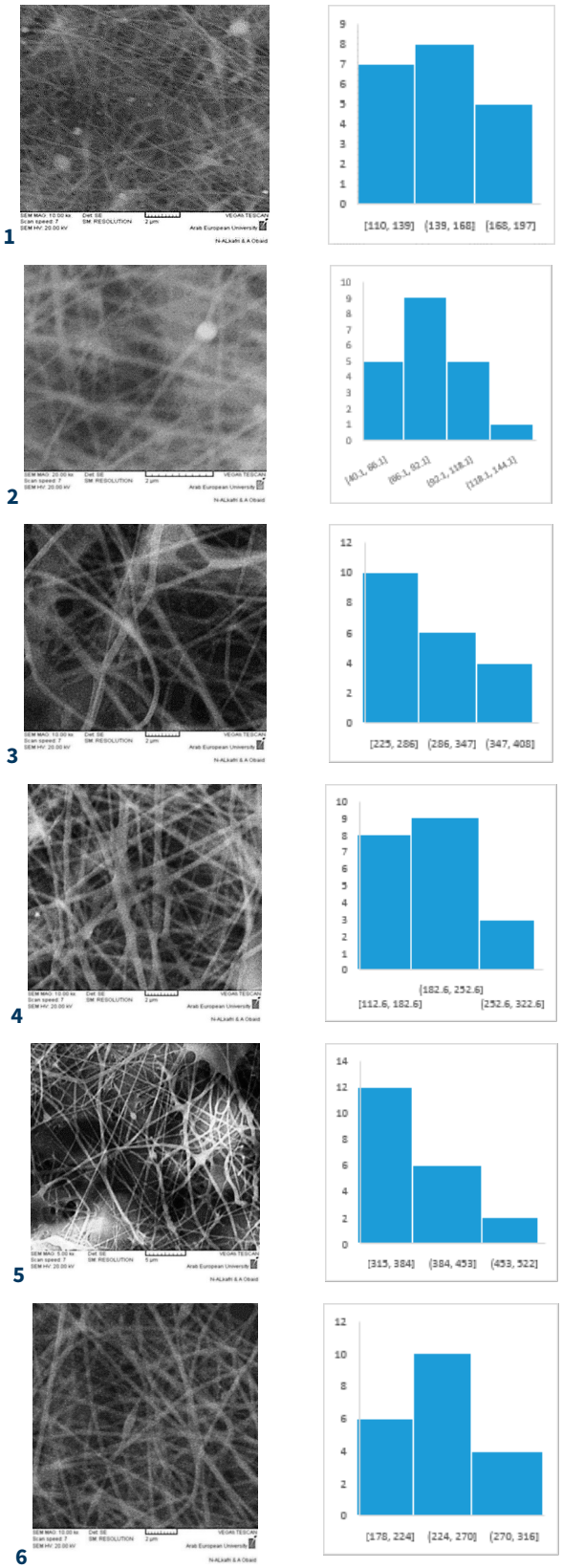

Figure 8. SEM images of the samples: 1: 10 GBD; 2: 10 SBD; 3: 15 GBD; 4: 15 SBD; 5: 30 GBD; 6: 30 SBD.

Table 4. Calculating diameters and their gradation.

Model	Fiber diameter range nm	Average diameter nm	deviation	Gradient amount nm
GBD	110-180.3	148.7	22.3	64.1
SBD	40.1-125.5	84.6	20.4	
GBD	225 -360	289.8	47.3	90
SBD	112.6-304.6	199.8	54.2	
GBD	315-517	390	53.2	151.1
SBD	178-295.7	238.9	35.9	

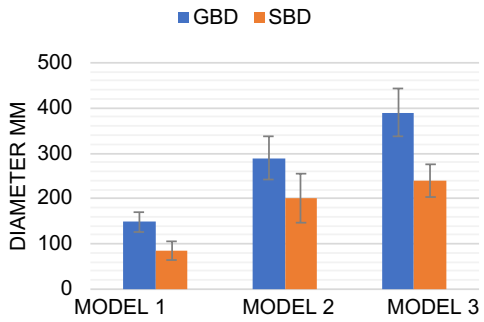

Figure 9. Comparison of fiber diameters taken from the two bases for each model.

From Figure 9, an increase in the diameters of the resulting fibers was observed as the conical surface inclination angle increased, reaching their largest value at the largest base of the third model, with an average of 390 nm. An increase in the range of the diameter gradation was also observed as the conical surface inclination increased.

A gradation in fiber diameters was obtained within a single sample between the largest and smallest bases for each conical collector model. This gradation resulted from the fact that the effect of the difference in the distance of the needle point from the collector surface at each extrusion moment was greater than the effect of the collector surface velocity, in addition to the electric field strength from the smallest base side, according to the Needle effect. Therefore, the fibers with the smallest diameter were those taken from the smallest base side. Increasing the cone's tilt angle also increased the diameter of its largest base, thus significantly decreasing the distance between the needle and the collector surface. This helped increase the distance between the needle and the collector. The increase in the diameters of the resulting nanofibers with increasing cone's tilt angle can be explained by a decrease in the accumulation of electrical charges on the cone's surface and, consequently, a decrease in the attractive force of the charge on the fiber, since the distribution of electrical charges on the collector surface decreases with increasing surface tilt.

A Statistical Study to Determine the Effect of the Difference in Fiber Diameter Between the Two Bases:

The results obtained in the microscopic gradation study of fiber samples show that there is a difference in the resulting fiber diameters along the length of the collector for each sample. To determine whether this difference is significant or not, professional statistics were utilized

Model 1

Anova: Single Factor

SUMMARY

Variance	Average	Sum	Count	Groups
418.3452	84.646	1692.92	20	ق.صغرى
501.2199	148.775	2975.5	20	ق.كبرى

ANOVA

F crit	P-value	F	MS	df	SS	Source of Variation
4.098172	1.57E-11	89.44508	41125.29	1	41125.29	Between Groups
			459.7825	38	17471.74	Within Groups
				39	58597.02	Total

Model 2

Anova: Single Factor

SUMMARY

Variance	Average	Sum	Count	Groups
2242.428	289.845	5796.9	20	ق كبرى
2945.435	199.875	3997.5	20	ق صغرى

ANOVA

F crit	P-value	F	MS	df	SS	Source of Variation
4.098172	2.1E-06	31.20592	80946.01	1	80946.01	Between Groups
			2593.931	38	98569.39	Within Groups
				39	179515.4	Total

Model 3

Anova: Single Factor

SUMMARY

Variance	Average	Sum	Count	Groups
2834.261	390.88	7817.6	20	ق كبرى
1292.336	238.905	4778.1	20	ق صغرى

ANOVA

F crit	P-value	F	MS	df	SS	Source of Variation
4.098172	6.96E-13	111.9392	230964	1	230964	Between Groups
			2063.298	38	78405.34	Within Groups
				39	309369.3	Total

Figure 10. Results of the statistical study of the three models: 1: 10; 2: 15; 3: 30.

using the program Excel, using the statistical function ANOVA (Maan, 2016). The results are shown in Figure 10.

From the Excel results, we find that for the first model, in the "Between Groups" field, which means the difference in diameter values between the two bases, we note that the variance value (MS) is greater than the variance

value for the "Within Groups" field. This means that there is a clear difference between the diameters taken from the larger base and the diameters taken from the smaller base. To determine whether this difference can be taken into account, we look at the P-value for the first field, which is equal to 15. This is much smaller than the value of , the significance level at $\alpha = 0.05$ (Excel). Therefore, the initial hypothesis is rejected, and the alternative hypothesis, which states that there is a fundamental difference between the average diameters taken from each of the two bases, is accepted. Similarly, for the second and third models.

The density calculation method at the nanoscale was also applied to the samples of the three cone models. The results are shown in Table 5 and Figure 11.

Table 5. Results of calculations of the surface density of fibers.

Model	Surface slope angle	Density fiber/5µ	
		Great base direction (GBD)	Small base direction (SBD)
1	10	10	10
2	15	8	9
3	30	8	8

It is noted in Figure 11 that the fiber density taken from the larger base side was very close to that taken from the smaller base side. This means that the angle of inclination of the cone's tip showed no significant effect on the density of the resulting meshes. It can be argued that the effect of the collector's rotational speed on fiber density was equivalent to the effect of the electrical charge distribution across the fibers.

3.2. Effect of Rotational Speed On Fiber Orientation and Alignment:

This study was conducted using the first conical collector model (10-degree inclination angle).

In Figure 12, we observe that at rotational speeds of 0 rpm and 1500 rpm, the fibers are randomly arranged, without any alignment, consistent with previous studies. In the third sample, taken at a rotational speed of 3000 rpm, some fibers started to align in a specific direction, although this was only a small percentage compared to the remaining random fibers. The image also indicates that some defects began to take on a spindle shape, whereas in the first and second samples, they were spherical. At a rotational speed of 4500 rpm, the alignment and parallelism of the fibers became noticeably clearer, with

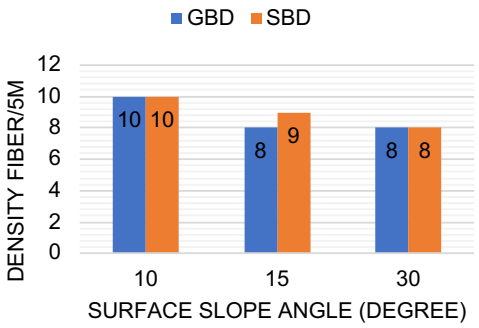

Figure 11. Results of calculations of the surface density of fibers.

a reduction in defects. By 6000 rpm, the fibers displayed significant orientation and complete parallelism among some of them.

Then, a study was conducted to measure the fiber tilt angles from each other for samples 3, 4, and 5 using the ImageJ program.

From Figure 13, it can be observed that the gray columns represent a deviation of less than 30 degrees. At a speed of 3000 rpm, several fibers exhibited a deviation of less than 15 degrees. At 4500 rpm, approximately 80% of the fibers had a deviation of less than 30 degrees, while at 6000 rpm, the majority of fibers also showed a deviation of less than 30 degrees. This indicates that an increase in the collector's rotational speed correlates with a higher number of fibers exhibiting minimal deviation from one another. In conclusion, higher rotational speeds of the collector (4500 rpm and above) resulted in better alignment and orientation of the resulting nanofibers, while other electrospinning process parameters remained constant. This orientation can be attributed to the fact that the fibers reach the collector's surface when its speed is high, which pulls the fibers in the direction of rotation, thus promoting parallelism.

Figure 14 illustrates the relationship between increasing rotational speed and the number of fibers with a deviation of less than 15 degrees. The linear velocities of the collector surface were calculated based on the larger base dimensions, which measured 24.2 mm and 66.5 mm. It was found that about 82% of the fibers were aligned in this manner.

No fiber orientation was observed in the images taken from the small base side of the conical complex, regardless of the change in rotational speed. This lack of orientation can be explained by the surface velocity at the small base, which was insufficient to induce orientation; the highest recorded value was 7.6 m/s. In contrast,

orientation began to occur from the large base side when the surface velocity reached 10.4 m/s, corresponding to 3000 revolutions per minute (rpm) “Figure 15”.

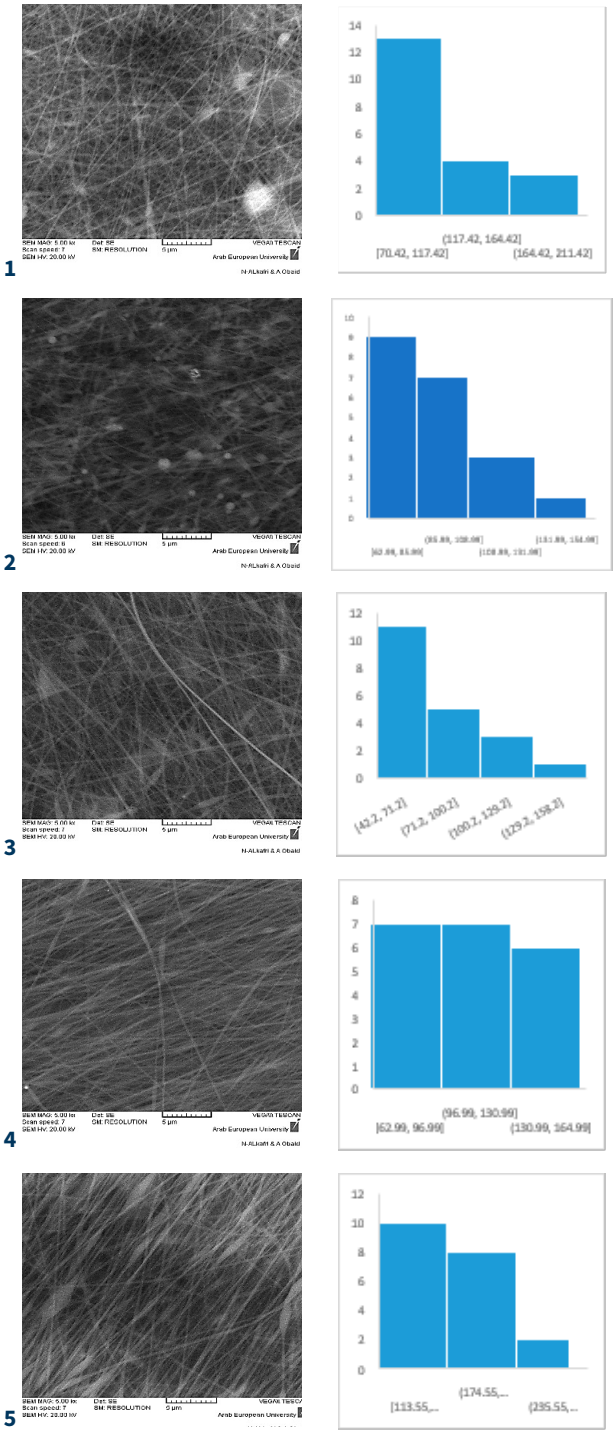

Figure 12. Pictures of samples of the great base direction of the conical collector: 1) 0 rpm; 2) 1500 rpm; 3) 3000 rpm; 4) 1500 rpm; 5) 6000 rpm.

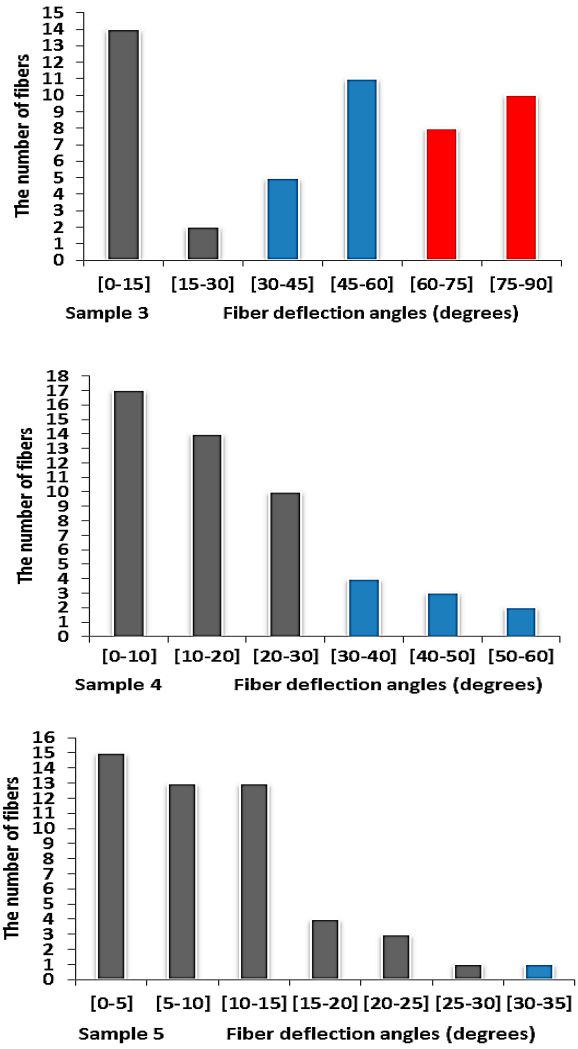

Figure 13. Number of oriented fibers with their inclination angles for the three samples: 3: 3000 rpm; 4: 1500 rpm; 5: 6000 rpm.

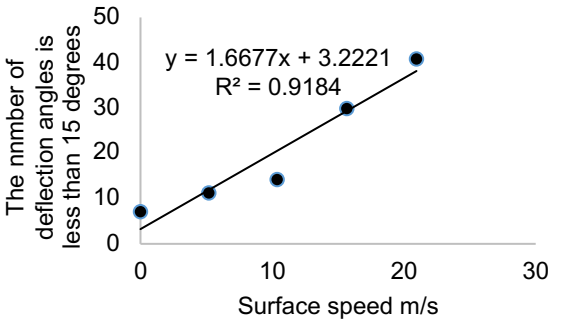

Figure 14. The relationship between the increase in rotational speed and the number of directed fibers.

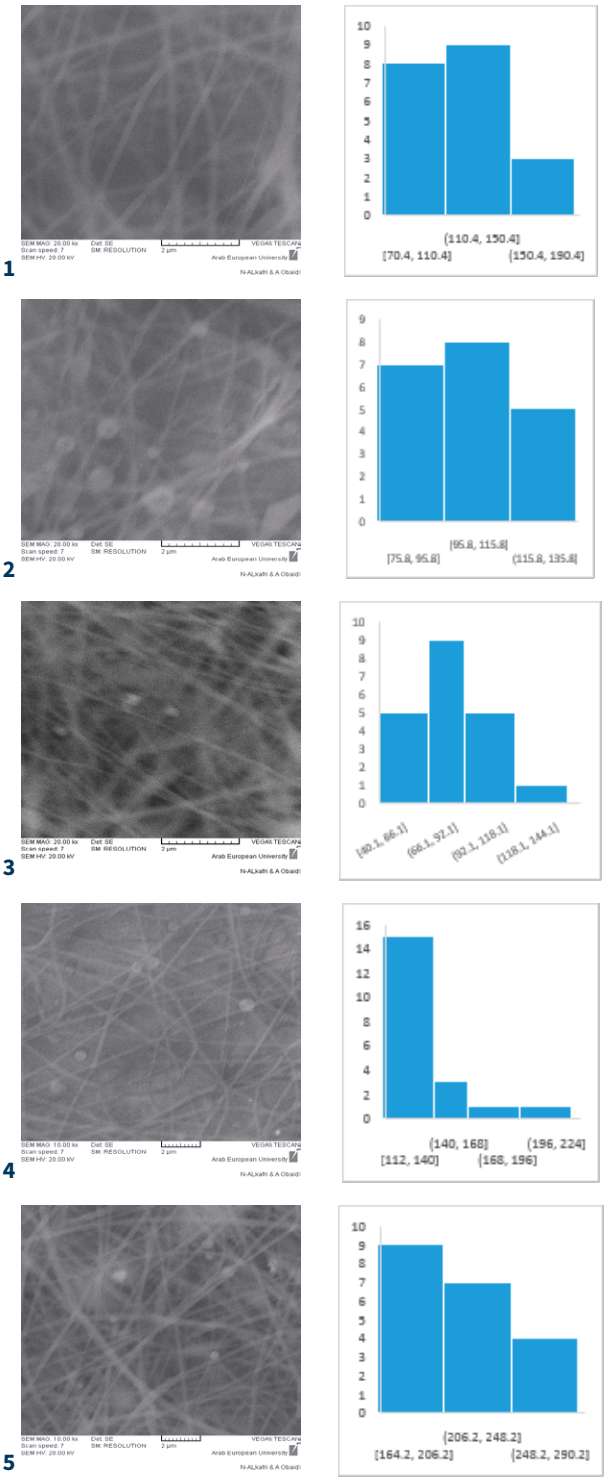

Figure 15. Pictures of samples of the small base direction of the conical collector: 1) 0 rpm; 2) 1500 rpm; 3) 3000 rpm; 4) 1500 rpm; 5) 6000 rpm.

The alignment gradient within a single sample along the cone was examined, starting from the small base and extending to the large base. This analysis is essential for determining the linear velocities that contribute to steering. Sample No. 5 was selected for this study, and five adjacent sections were taken from it at varying diameters of the manifold, as shown in Figure 16.

The alignment gradient in Sample No. 5 was mathematically expressed by calculating the deflection angles of 50 fibers. This measurement was taken at a diameter of 48.9 mm for the manifold, where the routing began.

Figure 16 shows a gradual change in fiber alignment along the sample. Starting from the small base, where the fibers were randomly oriented, they began to align in parallel at a diameter of 48.9 mm. The highest level of alignment was achieved at a diameter of 66.5 mm, as shown in Figure 17, which supports the previous findings.

Figure 18 indicates that as the collector surface velocity increases from 7.6 to 20.9 m/s, the fiber orientation also improves. This results in a significant increase in alignment, reaching a maximum of 82% alignment.

3.3. Effect of Rotational Speed On Fiber Diameters:

The diameters of 20 fibers from each sample taken from the two bases were measured, and their arithmetic mean was calculated using the image processing program | image. The results are shown in Tables 6 and 7.

Table 6. Calculation of the diameters of the major base fibers at the studied speed values.

Sample	Rotational speed rpm	Field fiber diameters	Average diameters	Deviation standard
1	0	85.6 -211.2	119.5	36.21
2	1500	62.9 – 133.6	93.1	17.99
3	3000	50.07 – 133.6	77.2	22.46
4	4500	62.9 – 159.3	110	26.41
5	6000	113.5 - 296	180.8	47.01

Table 7. Calculation of the diameters of the smallest base fibers at the studied speed values.

Sample	Rotational speed rpm	Field fiber diameters	Average diameters	Deviation standard
1	0	70.4 – 187.1	123.1	30.9
2	1500	75.8 – 129.8	101.7	15.86
3	3000	40.1 – 125.5	84.6	20.45
4	4500	112 - 240	168	38.19
5	6000	164.2 – 277.4	215.5	32.9

As shown in Figure 19, at the main base of the collector, at a rotational speed of 0 rpm, the average fiber diameter in the sample was 119.5 nm. As the rotational speed

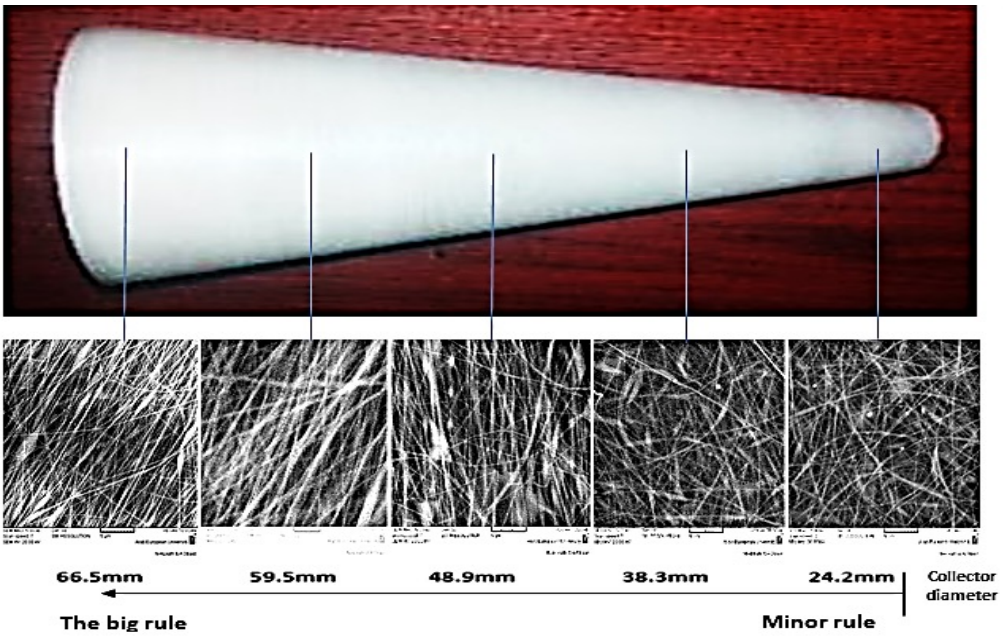

Figure 16. Alignment gradient within sample 5.

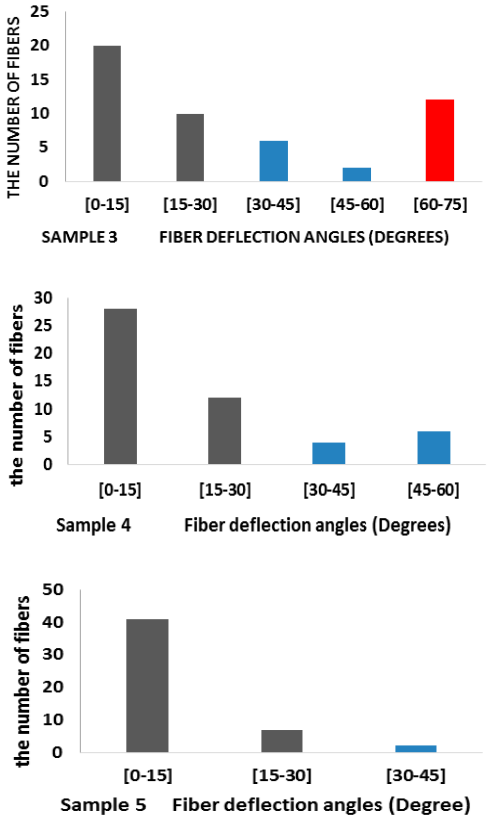

Figure 17. Deviation plots for the three gradient samples: sample 3: 48.9 mm; sample 4: 59.5 mm; sample 5: 66.5 mm.

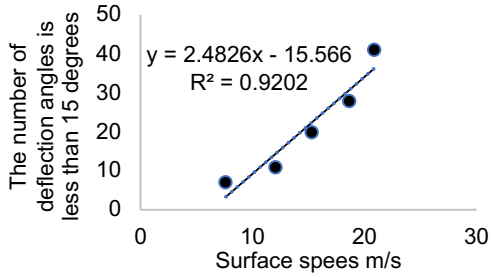

Figure 18. The relationship between surface velocity and the number of directed fibers in sample 5.

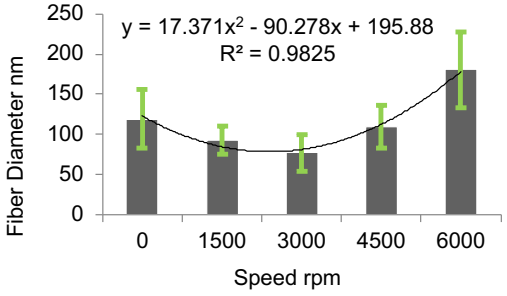

Figure 19. Relationship between the rotational speed of the collector and the diameters of the resulting nanofibers at the largest base.

increased to 1500 rpm, the average fiber diameter decreased to 93.1 nm, accompanied by a reduction in the standard deviation of the sample's diameters. At 3000 rpm, the average diameter decreased further to 77.2 nm, with the smallest diameter recorded at 50.07 nm. However, when the speed was increased from 3000 to 6000 rpm, the diameters of the resulting fibers increased to 180.8 nm, along with a larger standard deviation in the diameter values.

From this, we conclude that varying the collector's rotational speed significantly affects the diameters of the resulting nanofibers. The smallest observed diameter at a medium rotational speed of 3000 rpm indicates that the fibers were stretched, contributing to their elongation and reduced diameter. At this speed, the centrifugal force generated by the rotation did not have a noticeable effect, making it the most suitable speed for producing nanofibers with very small diameters. In contrast, at higher rotational speeds, the effect of force became apparent; the centrifugal force counteracted the attractive force acting on the charged fibers, leading to an increase in the diameters of the resulting fibers.

According to Figure 20, the results align with those obtained from samples taken from the large base side, where a rotational speed of 3000 rpm produced fibers with very small diameters, down to 40.1 nm. The relationship between speed and fiber diameter was established using the trend-line equations shown in Figures 19 and 20, enabling prediction of fiber diameter from the collector's operating rotational speed.

The difference between the diameters of the fibers taken from the side of the larger base of the collector and the diameters of the fibers taken from the side of the smaller base was evaluated, and the extent of the gradation of the fiber diameter along the cone was calculated. Figures 21 and 22 show the results of the diameter gradation.

As the rotational speed of the collector increased, its surface speed increased, and since the surface speed is related to the diameter of the collector, the diameters of the fibers taken from the side of the larger base (where the surface speed is higher) were smaller than the diameters of the fibers taken from the side of the smaller base.

A statistical study was conducted using ANOVA to determine whether the gradation of fiber diameters was effective. The study showed that the P-value for the fourth sample was 0.004 and for the fifth sample was 0.01 Figure 23. Both are smaller than the significance level, thus accepting the alternative hypothesis that there is a clear difference between the average diameters taken

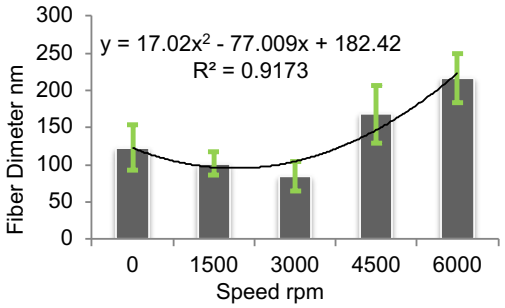

Figure 20. Relationship between the rotational speed of the collector and the diameters of the resulting nanofibers at the smallest base.

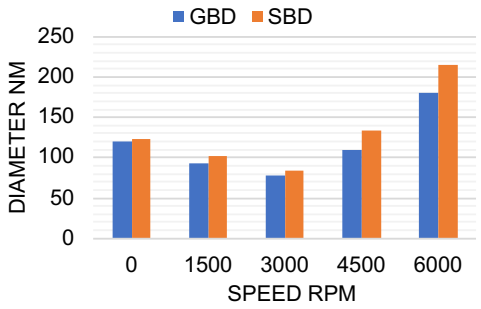

Figure 21. Results of the gradation in diameter.

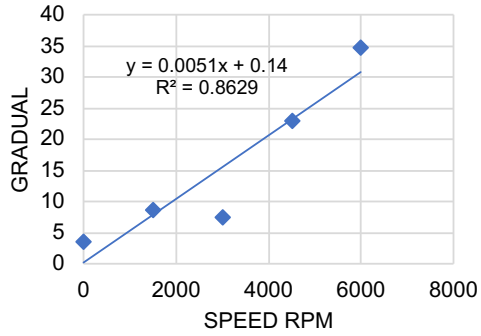

Figure 22. Speed-gradient relationship.

from each of the two bases. Therefore, the high rotational speed of the collector (4500 rpm and above) led to the emergence of a clear, substantial gradation in diameters between the two ends of the collector.

3.4. Effect of Rotational Speed On the Surface Density of Fibers:

The method for calculating density at the nanoscale, according to references, is done by drawing a straight

A

Anova: Single Factor

SUMMARY

Variance	Average	Sum	Count	Groups
697.5567	110.0385	2200.77	20	كبرى
480.0757	132.925	2658.5	20	صغرى

ANOVA

F crit	P-value	F	MS	df	SS	Source of Variation
4.098172	0.00497	8.895678	5237.919	1	5237.919	Between Groups
			588.8162	38	22375.01	Within Groups
				39	27612.93	Total

B

Anova: Single Factor

SUMMARY

Variance	Average	Sum	Count	Groups
2210.817	180.809	3616.18	20	كبرى
1084.977	215.519	4310.38	20	صغرى

ANOVA

F crit	P-value	F	MS	df	SS	Source of Variation
4.098172	0.010195	7.311041	12047.84	1	12047.84	Between Groups
			1647.897	38	62620.08	Within Groups
				39	74667.92	Total

Figure 23. Statistical study results: A: 4500rpm, B: 6000rpm.

horizontal line in the middle of the microscopic image of each sample and calculating the number of fibers that intersect with this line within a certain distance that is chosen (Zhou & Tan, 2017). This method was applied to microscopic images within a distance of 5 μm. The results are shown in Table 8.

Table 8. Results of surface density calculations.

rotational speed rpm	Density fiber/5µ		Gradual fiber
	Great base direction (GBD)	Great base direction (GBD)	
0	15	10	5
1500	13	9	4
3000	13	8	5
4500	14	6	8
6000	17	8	9

We note from Figure 24 that the effect of the surface velocity resulting from the collector's rotational speed on fiber density varied. The highest fiber density was at 6000 rpm, but the difference in density between the two ends of the collector for each sample was clear, as samples taken from the larger base side had a higher density than those taken from the smaller base side. We also note that the density gradient increased with increasing rotational speed. The reason for these results is the dual effect of the high surface velocity and the distance between the needle tip and the collector.

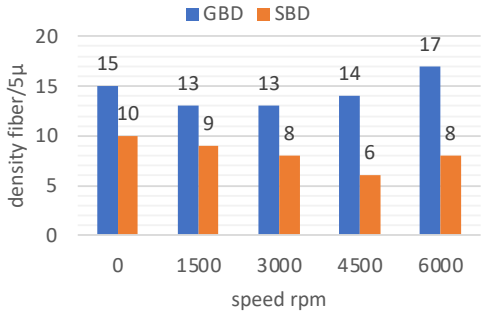

Figure 24. Effect of surface velocity on fiber density.

The fiber density was greatest from the larger base side, where the surface velocity was greater and the needle was closer to the collecting surface. It then gradually decreased along the length of the collector as the distance between the needle and the collector increased and the surface velocity decreased, reaching its lowest value at the smaller base of the collector.

It appears that the difference between the values expressing density is small, but the adopted nanoscale must be taken into account. Converting the adopted scale to fiber/mm (or fiber/cm) will make this difference significant at the sample level.

4. Conclusions

The importance of this study lies in the ability to predict the diameter, alignment, and density of the resulting fibers to obtain smaller, more homogeneous fiber networks according to the required specifications. This allows them to be used in various applications, especially three-dimensional fibers.

The study showed that increasing the cone tip tilt angle led to a greater increase in the diameter gradient of the electrospinning nanofibers between the two ends of the collector compared to the gradient resulting from increasing the rotational speed. This was accompanied by an increase in the diameters of the resulting fibers due to a decrease in the accumulation of electrical charges on the collector surface. However, there was no significant effect of varying the cone tip tilt angle on the density of the resulting fibers

It was also found that the collector's rotational speed controls the degree of fiber alignment, density, diameters, and gradation, thus achieving a three-dimensional structure. Increasing the operating speed gradually increases the probability of obtaining oriented fiber networks by 82%, depending on both the collector's rotational speed and the collector's diameter. A comparison between the

two collector bases also showed a gradation in alignment and diameters with varying speeds. The fiber diameter decreased to its smallest value on the nanoscale in the 3000-4500 rpm speed range, accompanied by an increase in density. The diameters then increased, and the density decreased in the 4500-6000 rpm speed range in both samples taken from the two bases. The derived relationship is useful in controlling the diameters of the fibers to be produced before starting the production process. These results will help in achieving nanoscale networks that may contribute to the development of the nanoelectronics industry and improve the growth sites of living cells in three-dimensional tissue engineering applications

5. Acknowledgment

The authors would like to express their gratitude to the Department of Textile Engineering, Petroleum and Chemical Engineering faculty, of Al Baath University for their valuable assistance.

6. Funding

The authors received no specific funding for this work.

7. Conflict of Interest

The authors declare that they have no conflicts of interest to disclose

8. Contributions of Authors

S. H. Conception, design and implementation of experiments in the laboratory, analysis and discussion of results, and G. T. proofreading and revision of results of microscopic processing of fabrics and K. A. proofreading and revision of calculations.

9. References

Ahmadi Bonakdar, M., & Rodrigue, D. (2024). Electrospinning: processes, structures, and materials. *Macromol*, *4*(1), 58-103. https://doi.org/10.3390/macromol4010004

Baede, T. A. (2009). *Towards a new position-controlled electrospinning setup* (Doctoral dissertation).

Bhardwaj, N., & Kundu, S. C. (2010). Electrospinning: A fascinating fiber fabrication technique. *Biotechnology advances*, *28*(3), 325-347. https://doi.org/10.1016/j.biotechadv.2010.01.004

Brown, P., & Stevens, K. (Eds.). (2007). *Nanofibers and nanotechnology in textiles*. Elsevier. https://books.google.com.mx/books?hl=es&lr=&id=iaujAgAAQBAJ&oi=fnd&pg=PP1&dq=Brown,+P.+J.+and+Stevens,+K.+(2007).+Nanofibers+and+nanotechnology+in+-textiles,+Woodhead+publishing+limited,+Cambridge,+England.+++&ots=_9jFQty6RJ&sig=z_0o2__ho5Qh8k_b1BBBDRMdieg&redir_esc=y#v=onepage&q=Brown%2C%20P.%20J.%20and%20Stevens%2C%20K.%20(2007).%20Nanofibers%20and%20nanotechnology%20in%20textiles%2C%20Woodhead%20publishing%20limited%2C%20Cambridge%2C%20England.&f=false

Bosworth, L., & Downes, S. (Eds.). (2011). *Electrospinning for tissue regeneration*. Elsevier. https://books.google.com.mx/books?hl=es&lr=&id=hyFtAgAAQBAJ&oi=fnd&pg=PP1&dq=Electrospinning+-for+Tissue+Regeneration&ots=Lfexv6mbI_&sig=tAcXn6QDf4UbKExMc246otvy2fQ&redir_esc=y#v=onepage&q=Electrospinning%20for%20Tissue%20Regeneration&f=false

Camilla & juan, H. (2016). PHD thesis entitled –study of the formation of nanoparticle collagen fibers using an electrical support, Cornell University USA.

Cao, Y., Liu, W., Sun, J., Han, Y., Zhang, J., Liu, S., ... & Guo, J. (2006). A technique for controlling the alignment of silver nanowires with an electric field. *Nanotechnology*, *17*(9), 2378-2380. https://doi.org/10.1088/0957-4484/17/9/050

Chuangchote, S., & Supaphol, P. (2006). Fabrication of aligned poly (vinyl alcohol) nanofibers by electrospinning. *Journal of nanoscience and nanotechnology*, *6*(1), 125-129. https://doi.org/10.1166/jnn.2006.17916

Cui, W., Zhou, Y., & Chang, J. (2010). Electrospun nanofibrous materials for tissue engineering and drug delivery. *Science and technology of advanced materials*, *11*(1), 014108. https://doi.org/10.1088/1468-6996/11/1/014108

Czaplewski, D. A., Verbridge, S. S., Kameoka, J., & Craighead, H. G. (2004). Nanomechanical oscillators fabricated using polymeric nanofiber templates. Nano Letters, 4(3), 437-439. https://doi.org/10.1021/nl035149y

Çetinkaya, H., Özden-Gürcan, G., Öteyaka, M. Ö., Şahin, M., & Mağden, G. K. (2024). Effect of electrospinning parameters on the production of polyvinyl alcohol (PVA)/Collagen (Type I) nanofiber membranes and the use of an adaptive neuro-fuzzy inference system for evaluating nanofiber diameters. Journal of Polymer Research, 31(12), 358. https://doi.org/10.1007/s10965-024-04203-0

Druesedow, C. J. (2008). Pressure control system for the electrospinning process: Non-invasive fluid level detection using infrared and ultrasonic sensors (Master›s thesis, University of Akron).
https://etd.ohiolink.edu/acprod/odb_etd/etd/r/1501/10?clear=10&p10_accession_num=akron1217275502

Haghi, A. K. (2009). *Electrospun nanofibers research: Recent developments*. Nova Science Publishers, Incorporated.
https://www.researchgate.net/publication/331008274_Electrospun_Nanofibers_Research_Recent_Developments

Haghi, A. K. (2010). Electrospun nanofiber process control. *Cellulose Chemistry & Technology*, *44*(9), 343.
https://www.researchgate.net/profile/A-Haghi/publication/267405372_Electrospun_nanofiber_process_control/links/5d6d6c754585150886096cc7/Electrospun-nanofiber-process-control.pdf

Haider, (2016). Electrical Experiments, Department of Physics, College of Science, Al-Mustansiriya University, Baghdad, Iraq.

Kumar, P. (2012). *Effect of colletor on electrospinning to fabricate aligned nano fiber* (Doctoral dissertation).
https://fileserver-az.core.ac.uk/download/pdf/53188629.pdf

Lawrencetine & Cato, T (2014) Nanotechnology and Cell-Bearing Tissue Engineering, King Saud University Press, Riyadh, Saudi Arabia, p. 393.

Li, D., & Xia, Y. (2004). Electrospinning of nanofibers: reinventing the wheel?. Advanced materials, 16(14), 1151-1170.
https://doi.org/10.1002/adma.200400719

Li, Z., & Wang, C. (2013). Electrospinning technique and unique nanofibers. One–Dimensional nanostructures, 141, 145.
https://doi.org/10.1007/978-3-642-36427-3

Maan, A., (2016) Professional Statistics Using Excel, Third Edition, Sabr Center for Statistical Studies and Public Policy, pp. 48-52.

Ramakrishna, S., Fujihara, K., Teo, W. E., Lim, T. C., & Ma, Z. (2005). An Introduction to Electrospinning and Nanofibers.
https://doi.org/10.1142/5894

Rafiei, S., Maghsoodloo, S., Noroozi, B., Mottaghitalab, V., & Haghi, A. K. (2013). Mathematical modeling in electrospinning process of nanofibers: a detailed review. *Cellul. Chem. Technol*, *47*(5), 323-338.
https://d1wqtxts1xzle7.cloudfront.net/112908249/p.323-338-libre.pdf?1711915809=&response-content-disposition=inline%3B+filename%3DMathematical_modeling_in_electrospinning.pdf&Expires=1778681149&Signature=XTZgmShI7V9WG3GbNAIiAZBIOlh2Upg0VZtAMF6f-dLSVcVMG2BYW4tk7V1qElqUthllvmTo1jKXna8a6nPXEN-hxd22C6VGKrlaUGpnKtEDG2x5j7NipKqCBl0K8g-BYvK-fwmUdlZqhLoTMrHy-n9UPkBE8AZmSGm8IgmsnTACP-J~55WPdP14tnlxn2JWlZnBmk5-nBOODCJ6Rhov7fXuFh-vbw0zu8GaNo1q8lvBNPj8j-1zlbb2Sl6xyRq46VC5EKBPqgu-3jUtfpwIYMvIsQQ7WCULR7e2TJ3iX8xGHlNO9bLMbUCm8Er-L6rOH6lboKNeZd8C~xyJkZheqNK-r-H2g__&Key-Pair-Id=APKAJLOHF5GGSLRBV4ZA

Rebicek, J., Pokorny, M., Velebny, V., (2011), Aligned nano fiber deposition onto a patterned rotating drum collector by electrospinning, Brno, Czech Republic, EU, 21-23.

Reneker, D. H., Yarin, A. L., Fong, H., & Koombhongse, S. (2000). Bending instability of electrically charged liquid jets of polymer solutions in electrospinning. Journal of Applied physics, 87(9), 4531-4547.
https://doi.org/10.1063/1.373532

Subbiah, T., Bhat, G. S., Tock, R. W., Parameswaran, S., & Ramkumar, S. S. (2005). Electrospinning of nanofibers. Journal of applied polymer science, 96(2), 557-569.
https://doi.org/10.1002/app.21481

Sukpancharoen, S., Wijakmatee, T., Katongtung, T., Ponhan, K., Rattanachoung, N., & Khojitmate, S. (2024). Data-driven prediction of electrospun nanofiber diameter using machine learning: A comprehensive study and web-based tool development. *Results in Engineering*, *24*, 102826.
https://doi.org/10.1016/j.rineng.2024.102826

Wang, C., Hsu, C. H., & Lin, J. H. (2006). Scaling laws in electrospinning of polystyrene solutions. *Macromolecules*, *39*(22), 7662-7672.
https://doi.org/10.1021/ma060866a

Zhou, Y., & Tan, G. Z. (2017). Fabrication of nanofiber mats with microstructure gradient by cone electrospinning. *Nanomaterials and Nanotechnology*, *7*, 1847980417748478.
https://doi.org/10.1177/1847980417748478

Zuniga-Navarrete, C., Segura, S. J., Baidya, S., Narváez-Muñoz, C., Toscano, J. D., & Segura, L. J. (2024). Electrospinning Process Modeling: A Multi-Stage View. In *International Manufacturing Science and Engineering Conference* (Vol. 88117, p. V002T07A005). American Society of Mechanical Engineers.
https://doi.org/10.1115/MSEC2024-125011